

Metal-Complex-Decorated Homochiral Heterobimetallic Telluride Single-Stranded Helix

Qichun Zhang,[†] Xianhui Bu,[‡] Zhien Lin,[†] Maurizio Biasini,[§] W. P. Beyermann,[§] and Pingyun Feng^{*†}

Department of Chemistry, University of California, Riverside, California 92521, Department of Chemistry and Biochemistry, California State University, 1250 Bellflower Boulevard, Long Beach, California 90840, and Department of Physics and Astronomy, University of California, Riverside, California 92521

Received June 10, 2007

Solvothermal reaction of a mixture of Sn, Mn, and Te at 200 °C using teta as the solvent yields a novel inorganic–organic hybrid solid $[\text{Mn}(\text{teta})(\text{en})] \cdot [\text{Mn}(\text{teta})][\text{Mn}(\text{SnTe}_4) \cdot \text{Mn}(\text{teta})]$ (teta = triethylenetetramine and en = ethylenediamine; **1**), which has a homochiral single-stranded helical structure. The material is a semiconductor with a band gap of 0.88 eV and shows paramagnetic behavior between 2 and 300 K.

The chemistry of metal tellurides has become an increasingly active area of research¹ because as small-band-gap semiconductors they have applications in the preparation of photovoltaic materials and in IR detection devices.² Furthermore, metal tellurides (e.g., Bi_2Te_3) are also among the best materials for thermoelectric applications.^{3,4} In the past decade, a number of interesting molecular, one-dimensional, layered, and three-dimensional tellurides have been produced.^{5–8}

Recently, in situ generated metal complexes have been demonstrated to be useful as structure-directing agents in the metal–chalcogenide system under hydro- or solvothermal conditions.^{9–12} The use of metal complexes as structure-

directing agents has several distinct features. Among them, the most important one is the integration of the electronic, optical, and magnetic properties of metal complexes with the host inorganic framework, which helps to provide complementary properties and synergistic effects. From the synthetic and structural perspectives, the use of metal complexes enables a new level of control over the host composition and topology. This is, in part, because metal complexes can integrate both hydrophilic and hydrophobic structure-directing effects: its positive charge favors the formation of the charged and usually hydrophilic framework, whereas its usual hydrophobic surface (the carbon backbone of the ligand) tends to favor the more hydrophobic organic surface on the inorganic framework. Such an “amphiphilic” structure-directing effect may play a role in the formation of the title compound, in which negatively charged Mn–Te–Sn helical chains are decorated with pendent metal complexes at the outer surface of the helices.

Here, we report a heterobimetallic telluride, $[\text{Mn}(\text{teta})(\text{en})] \cdot [\text{Mn}(\text{teta})][\text{Mn}(\text{SnTe}_4) \cdot \text{Mn}(\text{teta})]$ (teta = triethylenetetramine and en = ethylenediamine; **1**; Scheme 1). Com-

* To whom correspondence should be addressed. E-mail: pingyun.feng@ucr.edu.

[†] Department of Chemistry, University of California.

[‡] California State University.

[§] Department of Physics, University of California.

- (1) (a) Kanatzidis, M. G. *Acc. Chem. Res.* **2005**, *38*, 361. (b) Wachter, J. *Eur. J. Inorg. Chem.* **2004**, 1367. (c) Smith, D. M.; Ibers, J. A. *Coord. Chem. Rev.* **2000**, *200–202*, 187. (d) Chivers, T. *J. Chem. Soc., Dalton Trans.* **1996**, 1185.
- (2) (a) Bube, R. H. *Annu. Rev. Mater. Sci.* **1990**, *20*, 19. (b) Kudryastev, A. A. *The Chemistry and Technology of Selenium and Tellurium*, 2nd ed.; Elkin, E. M., Translator; Collect's publishers: London, 1974. (c) Maier, H.; Hesse, J. *J. Cryst. Growth* **1980**, *4*, 145.
- (3) (a) Kim, D.-H.; Byon, E.; Lee, G.-H.; Cho, S. *Thin Solid Films* **2006**, *510*, 148. (b) Zhou, J.; Jin, C.; Seol, J. H.; Li, X.; Shi, L. *Appl. Phys. Lett.* **2005**, *87*, 133109.
- (4) Hsu, K. F.; Loo, S.; Guo, F.; Chen, W.; Dyck, J. S.; Uher, C.; Hogan, T.; Polychroniadis, E. K.; Kanatzidis, M. G. *Science* **2004**, *303*, 818.
- (5) (a) Ruzin, E.; Fuchs, A.; Dehnen, S. *Chem. Commun.* **2006**, 4796. (b) Ruzin, E.; Kracke, A.; Dehnen, S. *Z. Anorg. Allg. Chem.* **2006**, *632*, 1018. (c) Shreeve-Keyer, J. L.; Warren, C. J.; Dhingra, S. S.; Haushalter, R. C. *Polyhedron* **1997**, *16*, 1193. (d) Pirani, A. M.; Mercier, H. P. A.; Dixon, D. A.; Borrmann, H.; Schrobilgent, G. J. *Inorg. Chem.* **2001**, *40*, 4823.
- (6) Wang, C.; Bu, X.; Zheng, N.; Feng, P. *Angew. Chem., Int. Ed.* **2002**, *41*, 1959.

- (7) Trikalities, P. N.; Bakes, T.; Kanatzidis, M. G. *J. Am. Chem. Soc.* **2005**, *127*, 3910.
- (8) (a) Biradha, K.; Seward, C.; Zaworotko, M. J. *Angew. Chem., Int. Ed.* **1999**, *38*, 492. (b) Thushari, S.; Cha, J. A. K.; Sung, H. H.-Y.; Chui, S. S.-Y.; Leung, A. L.-F.; Yen, Y.-F.; Williams, I. D. *Chem. Commun.* **2005**, 5515. (c) Li, J.; Chen, Z.; Lam, K.-C. *Inorg. Chem.* **1997**, *36*, 684. (d) Li, J.; Chen, Z.; Emge, T. J.; Proserpio, D. M. *Inorg. Chim. Acta* **1998**, *273*, 255. (f) Zang, S. Q.; Su, Y.; Li, Y. Z.; Ni, Z. P.; Meng, Q. *J. Inorg. Chem.* **2006**, *45*, 174. (g) Brabdl, M.; Ebner, A.; Kubicki, M. M.; Mugnier, Y.; Watchter, J.; Vigier-Juteau, E.; Zabel, M. *Eur. J. Inorg. Chem.* **2007**, 994–1003.
- (9) (a) Kromm, A.; Sheldrick, W. S. *Acta Crystallogr., Sect. E* **2006**, *E62*, m2767. (b) Billing, G. D.; Lemmerer, A. *CrystEngComm* **2006**, 686. (c) Nenoff, T. M.; Thoma, S. G.; Provencio, P.; Maxwell, R. S. *Chem. Mater.* **1998**, *10*, 3077. (d) Lin, C.-H.; Wang, S.-L. *Inorg. Chem.* **2001**, *40*, 2918.
- (10) (a) Lii, K.-H.; Chen, C.-Y. *Inorg. Chem.* **2000**, *39*, 3374. (b) Lin, H.-M.; Lii, K.-H. *Inorg. Chem.* **1998**, *37*, 4220.
- (11) (a) Zheng, N.; Bu, X.; Feng, P. *Chem. Commun.* **2005**, 2805. (b) Zhou, J.; Bian, G.-Q.; Dai, J.; Zhang, Y.; Tang, A.-B.; Zhu, Q.-Y. *Inorg. Chem.* **2007**, *46*, 1541.
- (12) Chen, Z.; Wang, R.-J.; Li, J. *Chem. Mater.* **2000**, *12*, 762.

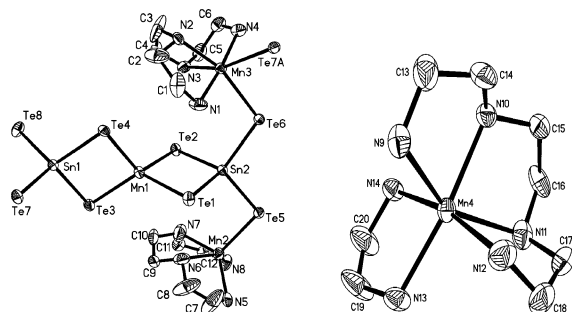
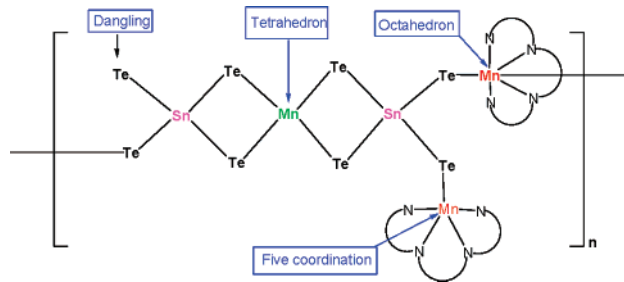


Figure 1. Thermal ellipsoid drawing (30% probability level) of [Mn(teta)-(en)]·[Mn(teta)][Mn(SnTe₄)₂·Mn(teta)].

Scheme 1. Polymeric Chain Structure of Compound **1**



Compound **1** consists of four unique Mn²⁺ sites, three of which exist in the metal complex form, as shown in Figure 1 and Scheme 1. An unusual observation is that these three metal complexes play distinctly different structural functions: (a) structure-directing in the isolated molecular form, (b) backbone-decorating as pendent species, and (c) cross-linking to form polymeric chains. The synergistic effect of these metal complexes helps to generate a single-stranded homochiral helix with the Mn–Te–Sn backbone, which is unprecedented among tellurides. The Mn–Sn–Te composition is of particular interest because the combination of magnetic and semiconducting elements has the potential to integrate magnetic and semiconducting properties in the same material.

To synthesize **1**, Sn (119 mg, 1.01 mmol), Mn (131 mg, 2.38 mmol), Te (508 mg, 3.98 mmol), and teta (70%, 3.108 g, 14.9 mmol) were combined in a 23 mL Teflon-lined stainless steel autoclave and stirred for 20 min. The sealed vessel was heated at 200 °C for 10 days. After cooling to room temperature, dark-red block crystals were obtained with about 82% yield (based on Sn).¹³ The structure was determined from single-crystal X-ray diffraction data collected at room temperature on an APEX II CCD diffractometer. The elemental analysis¹³ and Fourier transform IR data (Supporting Information) are consistent with the results obtained from single-crystal diffraction.

The structural analysis¹⁴ reveals that the inorganic–organic hybrid solid **1** crystallizes in the orthorhombic chiral space group $P2_12_12_1$ and has a single-stranded left-handed helical chain structure. Because all starting materials are achiral, the bulk product is expected to be a 50:50 racemic mixture consisting of crystals of different handedness. As shown in

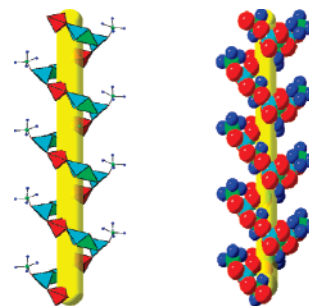


Figure 2. Polyhedral (left: Mn, red and green tetrahedra; Sn, cyan tetrahedron; Mn, green ball; N, blue ball) and space-filling (right: Te, red; Sn, cyan; Mn, green; N, blue) presentations of the left-handed single-stranded helix. C atoms are omitted for clarity.

Figure 1, the asymmetric unit consists of two crystallographically unique Sn⁴⁺ sites, four Mn²⁺ sites, eight Te²⁻ sites, and one en and three teta ligands. Both Sn⁴⁺ sites adopt tetrahedral coordination geometry (i.e., SnTe₄⁴⁻) and are linked together through edge-sharing with MnTe₄ to give a trimeric unit, SnTe₄MnSnTe₄. It is worth noting that the Te5 site on SnTe₄ is bonded to a terminal Mn(teta) group, while the Te8 site on SnTe₄ is dangling (Figure 1). All of the other six Te sites are bicoordinated between two Mn and Sn sites through either edge-sharing (Te1, Te2, Te3, and Te4) or corner-sharing (Te6 and Te7; Figure 1). The bond angles around the Sn⁴⁺ site range from 95.39(2)° to 116.95(2)°, and the Sn–Te bond distances are between 2.7007(7) and 2.7640(7) Å.

In comparison, the coordination chemistry of Mn²⁺ is far more diverse than that of Sn⁴⁺. The Mn–Te bond length ranges from 2.7470(7) to 2.9180(13) Å. There are four unique Mn²⁺ sites, each of which plays a unique structural role. Mn1 is similar to Sn⁴⁺ and is tetrahedrally coordinated to four Te atoms at the center of three edge-sharing tetrahedra, (SnTe₄)–Mn(SnTe₄) (Figure 1). Among four Mn²⁺ sites, Mn1 is the only one that is not bonded to the ligand. The Mn2 site is pentacoordinated to one Te atom and four N atoms from one teta molecule, and the Mn2(teta) group serves as a pendent group off of a SnTe₄ tetrahedron along the helical chain (Figure 2). Mn3 is octahedrally coordinated to two Te atoms and four N atoms from one teta, and this particular Mn3(teta) group serves as the two-connected link to join the trimeric unit (SnTe₄–Mn–SnTe₄, or more precisely [Mn–(SnTe₄)₂·Mn(teta)]) into an infinite chain. It should be noted that the structure contains no Sn–Te–Sn or Mn–Te–Mn linkages.

The octahedral Mn4 site is bonded to one teta molecule and one en molecule formed from the decomposition of the teta molecule during the synthesis. The molecular Mn4(teta)-(en) complex serves to balance the negative charge of the helix and also contributes to stabilization of the configuration and the stability of the helix.

(14) Crystal data: C₂₀H₅₈N₁₄Mn₄Sn₂Te₈, orthorhombic, space group $P2_12_12_1$ (No. 19), $a = 14.4563(2)$ Å, $b = 14.4726(2)$ Å, $c = 24.0551(4)$ Å, $V = 5032.81(13)$ Å³, $Z = 4$, $D_c = 2.604$ g/cm³, $F_{000} = 3568$, Mo K α radiation, $\lambda = 0.71073$ Å, $T = 293$ K, $2\theta_{\max} = 55.62$, 45 866 reflections collected, 9214 unique ($R_{\text{int}} = 0.0275$); final GOF = 0.950, $R1 = 0.0305$, $wR2 = 0.0712$, R indices based on 7952 reflections with $I > 2\sigma(I)$ (refinement on F^2), 433 parameters; absorption corrections applied, $\mu = 6.527$ mm⁻¹. Flack parameter = $-0.04(4)$.

(13) Elem. anal. Calcd: C, 12.17; H, 2.94; N, 9.94. Found: C, 12.39; H, 2.94; N, 9.04.

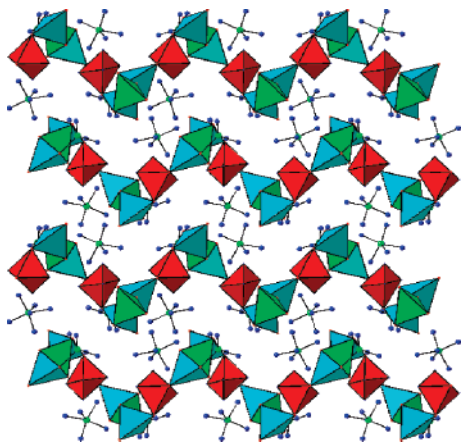


Figure 3. Parallel packing of adjacent single helices with the same chirality projected along the crystallographic b axis: Mn, red and green tetrahedra; Sn, cyan tetrahedron; Mn, green ball; N, blue ball. C atoms are omitted for clarity.

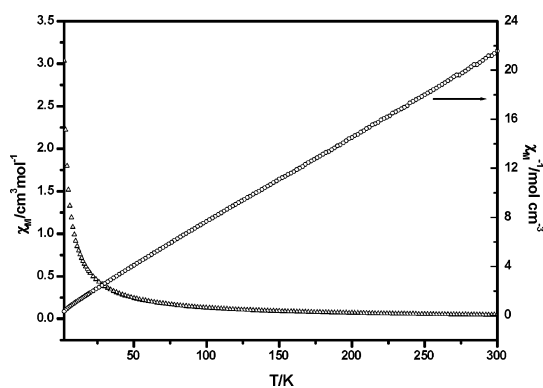


Figure 4. Temperature dependence of the magnetic susceptibility.

In **1**, all helices are of the same chirality (Figure 3) and are packed in a parallel manner, leading to a homochiral crystal. The helical pitch, given by the distance between equivalent atoms generated by one full rotation of the 2_1 axis, is equal to the periodicity along the crystallographic a axis, 14.4563(2) Å (Figure 2). To our knowledge, such a single-stranded helical configuration was not previously observed in metal tellurides.

The temperature dependence of the molar susceptibility showed Curie–Weiss behavior in the temperature range of 2–300 K (Figure 4). The data were fitted with $\chi_m = C_m/(T - \theta)$, where C_m and θ are the Curie and Weiss constants, respectively. The observed Curie constant ($C_m = 14.29 \text{ emu}\cdot\text{K}\cdot\text{mol}^{-1}$) corresponds to an effective paramagnetic moment of $\mu_{\text{eff}} = 10.55 \mu_B$, which is close to the spin-only value of $10.95 \mu_B$ for two Mn^{2+} (d^5) atoms. One possible explanation is that the spin orientations of the four unique Mn centers are different, with three Mn^{2+} atoms possessing $S = +5/2$ and one Mn^{2+} atom possessing the inverse spin $S = -5/2$.^{5a} It is also likely that electron pairing occurs at five- or six-coordinated Mn^{2+} sites because of the large d-orbital splitting. The exact nature of the magnetic coupling remains unknown. An antiferromagnetic interaction in tellurides at room temperature is not unusual, considering that MnTe is

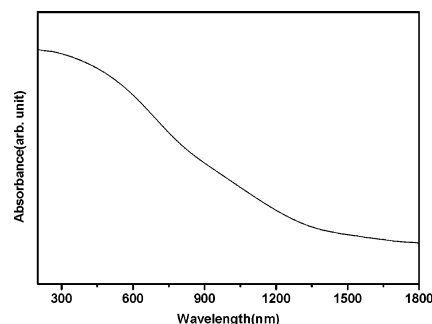


Figure 5. UV–vis absorption spectrum of compound **1**.

known to be an antiferromagnet with a Neel temperature of 323 K.¹⁵ The small negative Weiss constant ($\theta = -7.74 \text{ K}$) implies a weak antiferromagnetic coupling and is consistent with the observed paramagnetic behavior down to a very low temperature.

The diffuse-reflectance spectrum of compound **1** was studied on a Shimadzu UV-3101PC double-beam, double-monochromator spectrophotometer by using BaSO_4 powder as a 100% reflectance reference. As shown in Figure 5, the spectrum shows the absorption onset at about 1400 nm, indicating that compound **1** is a narrow-gap semiconductor with a band gap of 0.88 eV.

In summary, an inorganic–organic hybrid solid **1** featuring the polymeric Mn–Te–Sn structure is reported here. While the structure-directing role of the metal complex is well-known, the integration of multiple functions of metal complexes shown here (i.e., structure-directing, structure-decorating, and structure-building) is unprecedented. Such synergistic effects of metal complexes result in a single-stranded helix in a homochiral crystal that is rare among metal tellurides.

Acknowledgment. We are thankful for support of this work by the NSF (P.F.), the NIH (X.B.; Grant 2 S06 GM063119-05), Defense Microelectronics Activity (DMEA) under agreement number DOD/DMEA-CNN H94003-06-20604 (W.P.B. & M.B.), and the donors of the Petroleum Research Fund, administered by the American Chemical Society (X.B.; 41382-GB10). P.F. is a Camille Dreyfus Teacher–Scholar.

Note Added after ASAP Publication. This paper was released ASAP on August 1, 2007. Several corrections were made, and the correct version was posted on August 2, 2007.

Supporting Information Available: IR spectrum, experimental and simulated X-ray powder patterns, and crystallographic data including positional parameters, thermal parameters, and bond distances and angles (CIF). This material is available free of charge via the Internet at <http://pubs.acs.org>.

IC701135H

(15) Podgorny, M.; Oleszkiewicz, J. *J. Phys. C: Solid State Phys.* **1983**, *16*, 2547.